Journal of the European Ceramic Society **9** (1992) 231–242

Preparation and Characterization of Tape Cast Aluminum Nitride Substrates

T. Chartier, E. Streicher

URA CNRS 320, ENSCI, 47 av. Albert Thomas, 87065 Limoges, France

&

P. Boch

URA CNRS 302, ESPCI, 10 rue Vauquelin, 75231 Paris, France

(Received 8 May 1991; revised version received 18 July 1991; accepted 12 August 1991)

Abstract

This study was devoted to the preparation and characterization of tape cast AlN substrates. The tape casting conditions were selected to minimize the formation of defects, in particular during the burning out of organic phases. Al-, Si- and Ca-based oxides were studied as sintering additives. Small concentrations (0·5 wt%) of $CaCO_3$ or $3CaO–3SiO_2–Al_2O_3$ allow AlN materials to be sintered at rather low temperatures ($\leq 1650°C$). Thermal properties of AlN materials are very sensitive to the nature and location of secondary phases. The $Ca_2SiAl_2O_7$ phase and the 27R AlN polytype are detrimental to thermal conduction. $CaCO_3$ is the most favorable additive.

Diese Studie befaßt sich mit der Herstellung und der Charakterisierung bandgegossener AlN-Substrate. Die Bandguß-Bedingungen wurden so gewählt, daß möglichst wenige Defekte gebildet werden, insbesondere während des Ausbrennens organischer Phasen. Als Sinteradditive wurden Oxide auf Al-, Si- und Ca-Basis untersucht. Geringe Konzentrationen (0·5 Gew.%) an $CaCO_3$ oder $3CaO–3SiO_2–Al_2O_3$ ermöglichen das Sintern des AlN-Materials bei verhältnismäßig geringen Temperaturen ($\leq 1650°C$). Die thermischen Eigenschaften von AlN-Werkstoffen sind sehr empfindlich abhängig von der Art und Anordnung sekundärer Phasen. Die $Ca_2SiAl_2O_7$-Phase und das 27R AlN-Polytyp wirken sich nachteilig auf die thermische Leitfähigkeit aus. $CaCO_3$ ist das günstigste Additiv.

Cette étude est consacrée à la préparation et à la caractérisation de substrats AlN préparés par coulage en bande. Les conditions de coulage ont été choisies pour minimiser la formation de défauts, en particulier pendant la combustion des phases organiques. Des oxydes à base d'Al, Si et Ca ont été étudiés comme additifs de frittage. De faibles concentrations (0·5% en masse) en $CaCO_3$ ou $3CaO–3SiO_2–Al_2O_3$ permettent de fritter ces matériaux AlN à des températures relativement basses ($\leq 1650°C$). Les propriétés thermiques des matériaux décrits sont très sensibles à la nature et à la localisation des phases secondaires. La phase $Ca_2SiAl_2O_7$ et le polytype 27R AlN détériorent la conduction thermique. $CaCO_3$ est l'additif le plus favorable.

1 Introduction

The evolution of electronics toward more integration leads to a higher density of components. This density is limited by thermal dissipation and therefore high-conductivity substrates should be developed. The widely used alumina is not favorable from this point of view. BeO and SiC exhibit a high conductivity but the former is toxic, whereas the latter suffers from a high dielectric constant and high losses. Aluminum nitride seems to offer the best compromise between high thermal conductivity, low thermal expansion (close to that of Si), high electrical resistance and acceptable cost of fabrication. This study was devoted to the preparation of AlN substrates by tape casting and sintering, and their subsequent characterization.

Tape casting slurries are composed of ceramic

Journal of the European Ceramic Society 0955-2219/92/$5.00

powders dispersed in a solvent which contains dispersant, binder and plasticizer additions. Solvents allow powders to be deagglomerated and dispersed, and organic components to be dissolved. Common solvents are azeotropic mixtures such as 66–34 vol.% butan-2-one–ethanol[1–3] or 72–28 vol.% trichloroethylene–ethanol.[4–6] Dispersants favor the powder deagglomeration and avoid flocculation. Phosphate esters are effective dispersants in butan-2-one–ethanol.[1–7] Binders ensure the cohesion of green tapes after the solvent is evaporated.[8] They also increase the slurry viscosity.[9] Polyvinyl butyral and acrylic resins are common binders.[1–6] Most binders require the addition of plasticizers to improve the flexibility and workability of green tapes. Plasticizers partially break the bonds responsible for mechanical cohesion[10] and therefore decrease slurry viscosity.[9] Polyvinyl butyral binders are usually plasticized by glycols and/or phthalates, whereas acrylic binders are plasticized by phthalates. All organic components affect the rheological behavior of the slurry and therefore affect the properties of green tapes.

A slurry must be adjusted, taking into account powder characteristics, tape thickness and other processing parameters (e.g. thermocompression, pyrolysis and sintering parameters). Fiori & de Portu[4] have indicated some rules for the preparation of a tape casting slurry, namely: (i) the plasticizer to binder ratio must be less than 2; (ii) the amount of dispersant must be chosen in the range where the adsorption on the surface of particle is constant; (iii) the ratio between organic components and ceramic powder must be as low as possible; and (iv) the amount of solvent must be fixed at the minimum to ensure good dissolution of organic components and good homogenization of the slurry. An optimized slurry should lead to tapes which satisfy the following criteria: (i) no cracking during drying; (ii) good cohesion to allow the manipulation of dried sheets; (iii) good microstructural homogeneity; (iv) good thermocompression ability; and (v) easy pyrolysis. The optimization of tape casting slurries requires the close control of numerous parameters, with the particular aim of avoiding cracking during drying.

Densification of AlN materials is difficult. Three solutions are usually proposed to accelerate the densification kinetics:

(i) The use of AlN powders with a high specific surface area,[11–13] which promotes diffusion phenomena.
(ii) The use of hot-pressing or hot-isostatic-pressing,[14,15] which brings an external driving energy for densification.
(iii) The use of sintering aids, which leads to the formation of eutectic phases by reaction with AlN and allows liquid-phase sintering to take place. Common sintering aids are Y_2O_3[16–18] and CaO.[19–21]

AlN materials are generally sintered at temperatures around 1750°C. The use of high temperatures in a controlled atmosphere (nitrogen) is expensive, which could hinder the industrial development of AlN substrates. Therefore one aim of this study was to determine the conditions for obtaining rather dense materials at a sintering temperature as low as 1650°C. The influence of the nature and the quantity of sintering aids on the densification of AlN was studied. Calcium compounds were chosen because these yield eutectics in the Al_2O_3–CaO system and form liquid phases at low temperatures (1400°C; see Fig. 1). The paper also focuses on the sensitivity of thermal diffusivity to the nature and location of secondary phases.

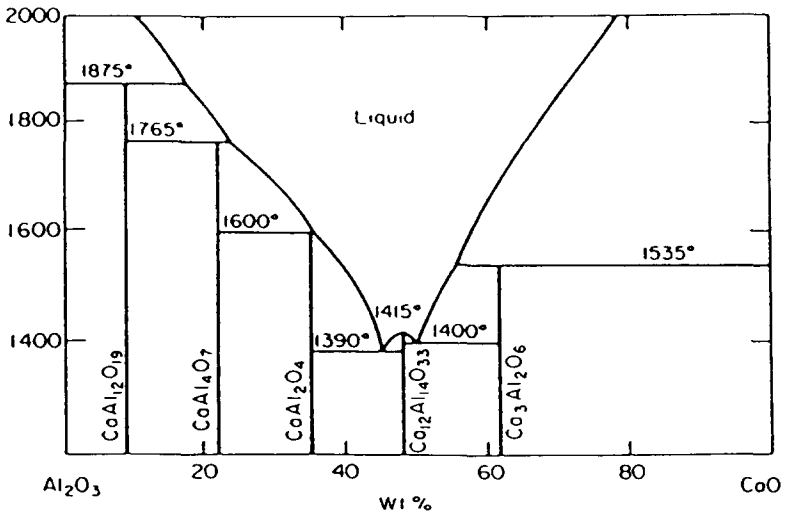

Fig. 1. Phase diagram for the system Al_2O_3–CaO.[22]

2 Experimental

2.1 Starting materials

The AlN powders (Starck, FRG) were of three grades (A, B and C) with a mean grain size of 8, 2 and 1·3 μm, respectively. These three grades exhibit similar particle size distributions and particle shapes. The sintering aids were Y_2O_3 (Rhône-Poulenc, France) and Ca-based compounds: $CaCO_3$ (C), $CaO–SiO_2$ (CS), $3CaO–3SiO_2–Al_2O_3$ (C3S3A) and $CaO–2SiO_2–Al_2O_3$ (CS2A). The two aluminates were prepared by ball milling and subsequent reactive calcination of $CaCO_3$ (Merck, FRG), SiO_2 (C800, Sifraco, France) and Al_2O_3 (A16SG, AlCoA, USA) mixtures. Compositions of AlN with the addition of 0·5, 1, 1·5, 2, 4 and 6 wt% for C, CS and C3S3A and of 2, 4 and 6 wt% for CS2A were studied.

The solvent was an azeotropic mixture of 66–34 vol.% butan-2-one–ethanol. The dispersant was a phosphate ester (C-213, CECA, France). The binder was a polyvinyl butyral (PVB). The plasticizer was a 50/50 wt% mixture of polyethylene glycol (PEG) and phthalate (PHT).

2.2 Sample preparation

Three parameters were chosen to characterize the tape casting slurry. The first was the inorganic to organic ratio (X), equal to the volume of powder divided by the total volume of powder, dispersant, binder and plasticizer. The second was the binder to plasticizer ratio (Y), equal to the volume of binder divided by the volume of plasticizer. The third parameter was the mean grain size of the powder (ϕ): 8, 2 and 1·3 μm for the A, B and C AlN grades, respectively. The slurry compositions are given in Tables 1 and 2. The C_{o3} composition (Table 1) was used to study the influence of grain size on cracking during drying. In all cases the viscosity of the slurry was kept at 800 mPa.s by adjusting the amount of solvent. Green tapes with a thickness of 200–300 μm were tape cast on a glass slab. The drying rate was measured for 200-mm long green tapes. Tape cracking was visually detected on 1-m long samples. 30-mm diameter disks were punched from tapes. Some of them were used for density–porosity measurements and others were thermocompressed to prepare 4-mm thick substrates, to study the thermocompression ability. Thermocompression was performed at 70 °C under a pressure of 60 MPa.

The sintering study was conducted using 10-mm diameter, 4-mm thick disks, stamped from the tapes and then thermocompressed. The tape composition was defined from the C_{o3} composition, where Y_2O_3 was replaced by calcium compounds. The pyrolysis of organic components and the sintering treatment

Table 1. Slurry compositions (X variable and $Y = 0·79$)

Component	*Density* ($g\,cm^{-3}$)	*Composition (vol.%)*					
		C_{o1}	C_{o2}	C_{o3}	C_{o4}	C_{o5}	C_{o6}
AlN (B), (C)	3·16	38·53	33·90	33·14	29·77	26·45	23·45
Y_2O_3	4·79	0·79	0·70	0·69	0·62	0·55	0·48
C-213	1·05	0·25	0·22	0·22	0·20	0·18	0·16
Solvent	0·82	52·86	54·59	53·38	53·27	55·22	55·96
PVB	1·10	3·35	4·68	5·62	7·14	7·74	8·82
PHT	1·05	2·19	3·06	3·52	4·67	5·11	5·77
PEG	1·13	2·03	2·85	3·43	4·33	4·75	5·36
X		0·83	0·76	0·72	0·65	0·60	0·54

Table 2. Slurry compositions (Y variable and $X = 0·76$)

Component	*Composition (vol.%)*								
	C_{b1}	C_{b2}	C_{b3}	C_{b4}	C_{b5}	C_{b6}	C_{b7}	C_{b8}	C_{b9}
AlN (B)	39·47				33·90				
Y_2O_3	0·81				0·70				
C-123	0·26				0·22				
Solvent	47·09				54·59				
PVB	2·82	3·50	4·68	5·27	5·91	6·35	6·67	6·83	7·00
PHT	4·94	3·68	3·07	2·76	2·43	2·20	2·03	1·95	1·84
PEG	4·59	3·41	2·84	2·56	2·25	2·04	1·89	1·81	1·75
Y	0·30	0·49	0·79	0·99	1·26	1·50	1·70	1·82	1·96

at 1650°C were carried out by Xeram Company (Pechiney, France).

2.3 Characterization

Tapes are bound to the glass slab during all the drying time. The slab is rigid and it can be considered that shrinkage operates mostly along the thickness of the tape, i.e. perpendicularly to its surface. The tape shrinkage during drying was measured by a laboratory-made detector using a laser system. The solvent evaporation was simultaneously measured by a balance connected to a computer. Two measurements of shrinkage and weight were performed for each composition.

The shrinkage (S) was determined from the S_t/T_f ratio, S_t being the shrinkage at time t and T_f the thickness after complete drying. Using a least-squares method, the evolution of shrinkage versus drying time was approximated by the relation

$$S(t) = a_1 \exp(b_1/t) \quad (1)$$

where a_1 and b_1 are constants.

The shrinkage rate (SR) was then calculated by differentiating eqn (1):

$$\mathrm{SR}(t) = T_f \, \mathrm{d}S(t)/\mathrm{d}t = -T_f a_1 \exp(b_1/t) b_1/t^2 \quad (2)$$

A two-stage process has been commonly observed for the drying of green tapes.[5,6] The first stage proceeds at a constant rate, so a convenient expression of the remaining amount of solvent (RS) at time t is

$$\mathrm{RS}(t) = a_2 t + b_2 \quad (3)$$

where a_2 and b_2 are constants. For longer times the evaporation rate decreases exponentially and a convenient expression is

$$\mathrm{RS}(t) = a_3 \exp(b_3/t) \quad (4)$$

where a_3 and b_3 are constants.

The drying rate (DR), at a given time (t_i), was calculated from the following expression:

$$\mathrm{DR}(t_i) = (W_{t_{i-1}} - W_{t_i})/(t_{i-1} - t_i) \quad (5)$$

where W_{t_i} is the weight at time t_i.

The knowledge of the variations of weight and shrinkage versus time allows the determination of the relative content of each component (powder, organic phase, porosity) of the tape at any time during drying. The total volume was taken as the sum of the volumes of ceramic powders, organic phases and pores.

The apparent densities of green samples, excluding organic phases, were determined by measuring the volume and weight of samples before and after calcination (V and V_{cal} for the volumes, M and M_{cal} for the weights). The apparent density is expressed by the M_{cal}/V ratio. Calculated X ratios given in Table 1 were confirmed by M and M_{cal} values.

The tensile strength was measured on dog-bone samples punched from green tapes. The loading cell sensitivity of the tensile machine was 0·1 N and the loading rate was 2 cm min^{-1}.

The apparent densities and open porosities of the sintered products were measured by Archimedes' method in water. The value of open porosity was the basic indicator for the extent of densification. Qualitative characterization of crystalline phases was performed by X-ray diffraction. Microstructural features were observed by TEM. Thermal diffusivity was measured using a laser flash method.

3 Results and Discussion

3.1 Tape casting

3.1.1 Cracking during drying

The tapes made with AlN of the B grade usually crack when X becomes greater than 0·76 (Table 3) whereas the tapes made with the C grade crack when $X > 0{\cdot}65$. As far as Y is concerned, cracking develops in grade B tapes for $Y > 0{\cdot}79$ (Table 4). For the C_{o3} composition ($X = 0{\cdot}72$, $Y = 0{\cdot}79$) cracking only appeared in the tapes made with the C grade. These data show that cracking during drying is sensitive to the three parameters chosen to characterize the slurries. The role of each of these parameters will be discussed later.

3.1.2 Shrinkage and evaporation

The drying of tape cast sheets has been studied by Mistler *et al.*[5] and Shanefield.[6] A two-stage process was commonly observed. In the first stage the slurry

Table 3. Cracking during drying for AlN (grades B and C) versus X

Grade	*Composition (value of X)*					
	C_{o1} (0·83)	C_{o2} (0·76)	C_{o3} (0·72)	C_{o4} (0·65)	C_{o5} (0·60)	C_{o6} (0·54)
AlN (B)	Cracked	←		No cracks		→
AlN (C)	Cracked	Slightly cracked	Slightly cracked	←	No cracks	→

Table 4. Cracking during drying for AlN (grade B) versus Y

Cracking	*Composition (value of Y)*								
	C_{b1} (0·30)	C_{b2} (0·49)	C_{b3} (0·79)	C_{b4} (0·99)	C_{b5} (1·26)	C_{b6} (1·50)	C_{b7} (1·70)	C_{b8} (1·82)	C_{b9} (1·96)
	← No cracks →			← Slightly cracked →				← Cracked →	

is still fluid and the solvent flows through the sheet by liquid diffusion or capillary action and evaporates at the surface at a constant rate. In the second stage the surface of the sheet solidifies and the diffusion of the solvent is slow, which reduces the drying rate. The migration of solvent and the shrinkage effects induce stress in the tape. Two cases can be distinguished: shrinkage stops in the course of the first stage of evaporation or continues during the second stage of evaporation. This second case is the less favorable and generally yields cracking.

The drying rate and the shrinkage rate are plotted in Figs 2 and 3. The shrinkage rate increases when X or Y increase, or when ϕ decreases (Fig. 3 and Table 5). A first stage of evaporation at a constant rate is not observed in the present experimental conditions (room temperature, air drying, 250-μm tape thickness). Only the second stage of evaporation was observed, with a drying rate continuously decreasing when time proceeds. Maybe the first stage was too short to be detected. According to comments by Mistler and Shanefield, this means that the risk of cracking is high. This study shows that cracking depends on shrinkage rate, which depends itself on the composition of the slurry. For low-X compositions the high content of organic phases slows down the motion of particles, then reduces the shrinkage rate. However, the binder role is bonding the ceramic particles together. Tensile tests have shown that the binder exhibits higher strength when unplasticized. The higher the binder content, the stronger the inter-particles link, the higher the shrinkage rate.

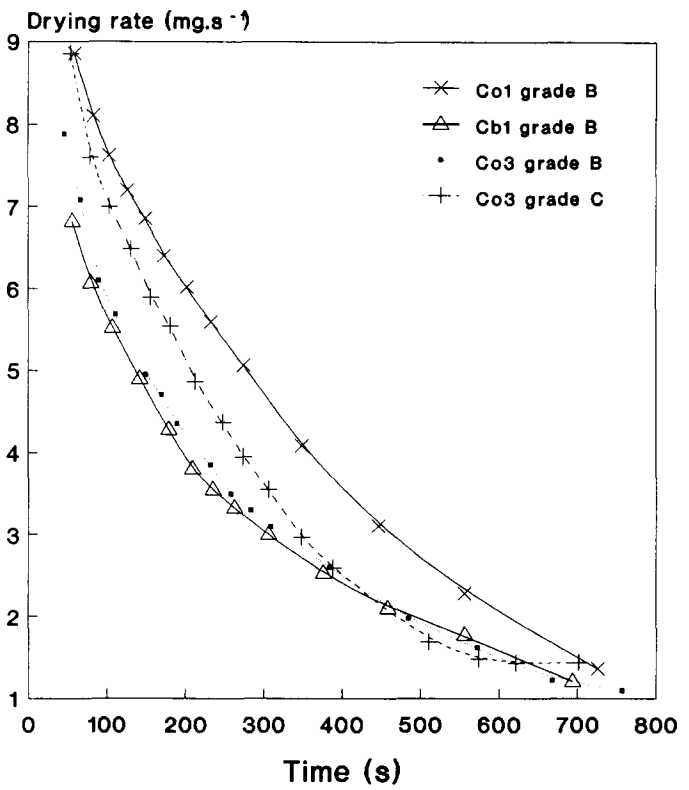

Fig. 2. Drying rate versus time for C_{o1}, C_{b1} (grade B) and C_{o3} (grades B and C).

The low shrinkage rate which is required to avoid cracking can be obtained combining the three following conditions: (i) a low value of X; (ii) a low value of Y; and (iii) a medium value of ϕ.

3.1.3 Microstructure

The microstructure of green tapes greatly influences the green properties but also the critical step of burning out with the formation of defects.[23] The nature and the distribution of the organic phase and the pore structure within the green sheets affect the removal of organic components.[24,25] The determination of the relative content of each component (powders, solvent, organic phase and pores) aids the understanding of the evolution of the tape microstructure during the drying period. The study has focused on porosity, which is the most significant

Table 5. Maximum shrinkage rate for various values of X and Y, and various grades of AlN

	Composition			*Maximum shrinkage rate* ($\mu m\,s^{-1}$)
	X	Y	*Grade*	
C_{o1}	0·83	0·79	B	0·88
C_{o2}	0·76	—	—	0·83
C_{o3}	0·72	—	—	0·78
C_{o4}	0·65	—	—	0·80
C_{o6}	0·54	—	—	0·79
C_{b1}	0·76	0·30	B	0·61
C_{b3}	—	0·79	—	0·83
C_{b6}	—	1·50	—	0·88
C_{b9}	—	1·96	—	1·13
C_{o3}	0·72	0·79	A	0·77
C_{o3}	—	—	B	0·78
C_{o3}	—	—	C	1·35

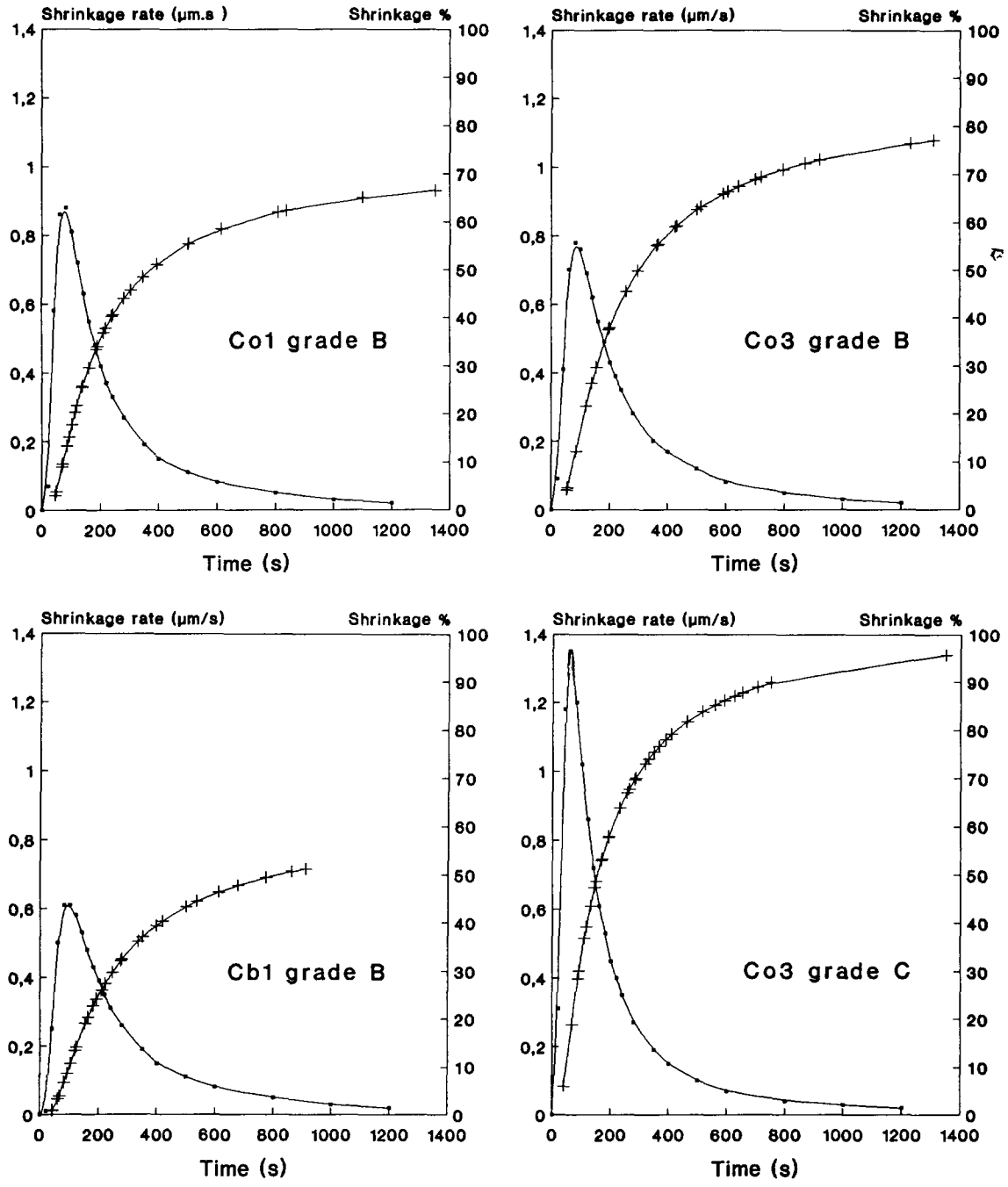

Fig. 3. Shrinkage and shrinkage rate during drying for C_{o1}, C_{b1} (grade B) and C_{o3} (grades B and C).

parameter. A first result is that porosity was not zero after casting: values as high as 20% were determined. Figures 4 and 5 show the evolution of porosity versus time for various values of X and Y. The porosity observed just after casting can be due to the presence of air bubbles entrapped during the casting of the slurry. At the beginning of the drying stage particles rearrange themselves and bubbles burst on the surface of the tape. The porosity decreases until the shrinkage stops, then increases again because of the removal of the remaining solvent. For $X > 0{\cdot}72$ porosity does not disappear completely during shrinkage. There is around 8% of residual porosity in the C_{o1} material ($X = 0{\cdot}83$). A similar behavior was observed in the case where Y is low: for $Y = 0{\cdot}3$ the residual porosity at the end of shrinkage in the C_{b1} material is around 7%.

The apparent density and porosity of dried tapes were determined for the three AlN grades, for various values of X and Y. The results are shown in Table 6. A schematic illustration of the influence of X and Y on the microstructure of green sheets is given in Fig. 6.

When X decreases the organic phases prevent particles from packing together, therefore both density and porosity decrease. Porosity is filled with

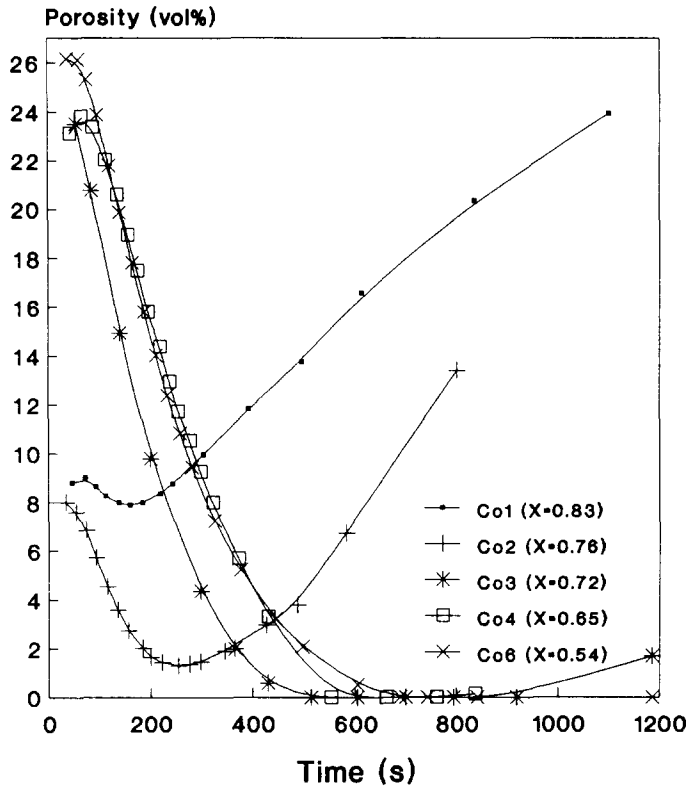

Fig. 4. Porosity versus time for various values of X.

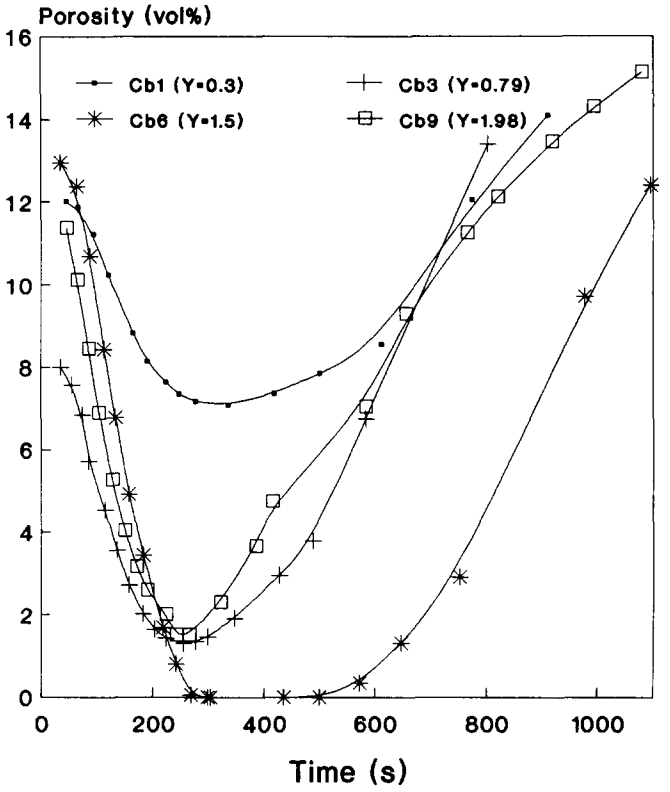

Fig. 5. Porosity versus time for various values of Y.

organic components. The evolution of the tape porosity versus time depends on X. For high values of X the ceramic particles are densely packed and their respective movements are too small to allow a complete elimination of porosity. Therefore the total shrinkage decreases when X increases.

Low-Y green tapes exhibit a higher density and a lower porosity than high-Y ones. After shrinkage the low viscosity of the plasticizer-rich organic phase allows it to flow between the grains and to fill in the pores, hence leading to low porosity samples. When Y increases the grain rearrangement is too small to allow complete removal of porosity.

The highest density was obtained in the tapes made with the B grade. The total shrinkage was maximum for the tapes made with the C grade. Figure 7 shows the variation of porosity versus drying time for the three AlN grades. The variations of porosity are similar whatever the grade. Porosity decreases to zero after 3–8 min of drying, then

Table 6. Total shrinkage, apparent density and porosity of dried tapes for various values of X and Y, and various AlN grades

	Composition			*Total shrinkage* (S_f/T_f)	*Density* ($g\,cm^{-3}$)	*Porosity* (*vol.%*)
	X	Y	*Grade*			
C_{o1}	0·83	0·79	B	0·57	1·98	26
C_{o2}	0·76	—	—	0·70	1·90	21
C_{o3}	0·72	—	—	0·76	1·87	20
C_{o4}	0·65	—	—	1·16	1·79	14
C_{o6}	0·54	—	—	1·40	1·66	4
C_{b1}	0·76	0·30	B	0·46	1·99	19
C_{b3}	—	0·79	—	0·70	1·90	21
C_{b6}	—	1·50	—	0·80	1·83	25
C_{b9}	—	1·96	—	0·92	1·81	26
C_{o3}	0·72	0·79	A	0·66	1·77	29
C_{o3}	—	—	B	0·76	1·87	20
C_{o3}	—	—	C	0·87	1·83	23

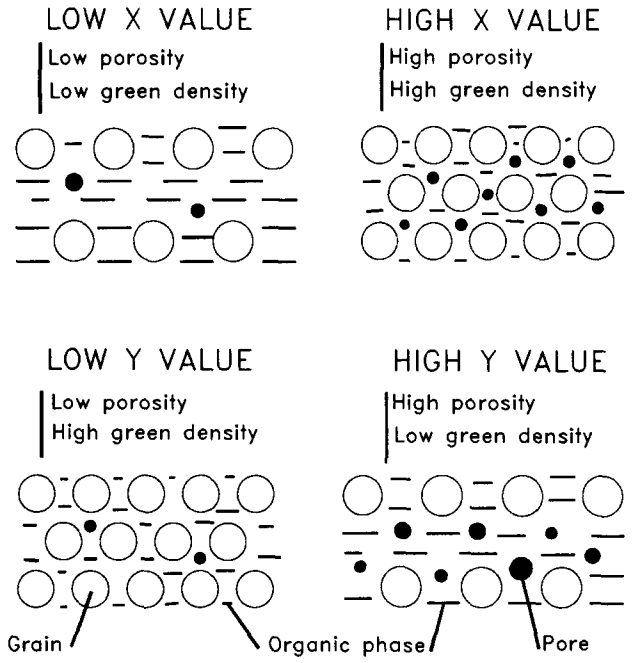

Fig. 6. Influence of X and Y on the microstructure of the green tapes.

increases to 20–29% after complete drying. B grade AlN leads to green products with higher densities than A and C grades. Similar results have been obtained for dry-pressed samples with no organic component: 1·82, 1·92 and 1·89 g cm^{-3} for AlN A, B and C, respectively, for a pressure of 160 MPa. Both coarse and very fine powders are difficult to compact.

3.1.4 Properties of green tapes

3.1.4.1 Tensile strength. Figure 8 shows that the tensile strength of green sheets does not vary with X, although the porosity increases as X increases. On the contrary, Fig. 9 shows that strength increases when Y increases.

3.1.4.2 Thermocompression ability. The thermocompression behavior of green sheets is sensitive to X and Y. The presence of delaminations was detected using an ultrasonic method. Delaminations were numerous in samples with low quantities of organic phases (C_{o1}, C_{o2} and C_{o3}), but they were rare in samples with high quantities of organic phases (C_{o4}, C_{o5} and C_{o6}).

A lot of delaminations were observed in samples with a high quantity of plasticizer (C_{b1}, C_{b2} and C_{b3}). On the contrary, samples with a high Y ratio (C_{b5} to C_{b9}), i.e. with a low quantity of plasticizer, do not exhibit any delamination. The plasticizer acts as a lubricant between the individual layers, which limits the bonding during thermocompression.

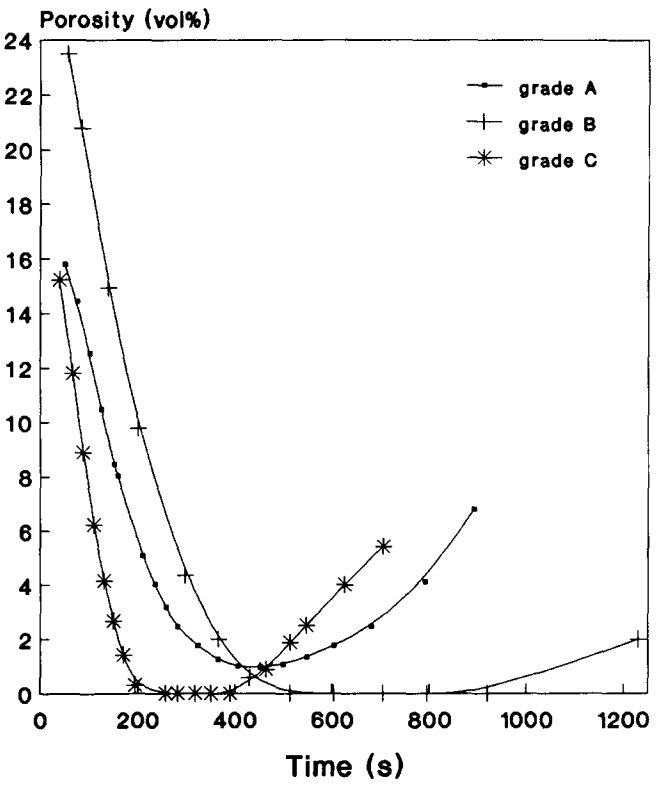

Fig. 7. Porosity versus time for grades A, B and C (C_{o3} composition).

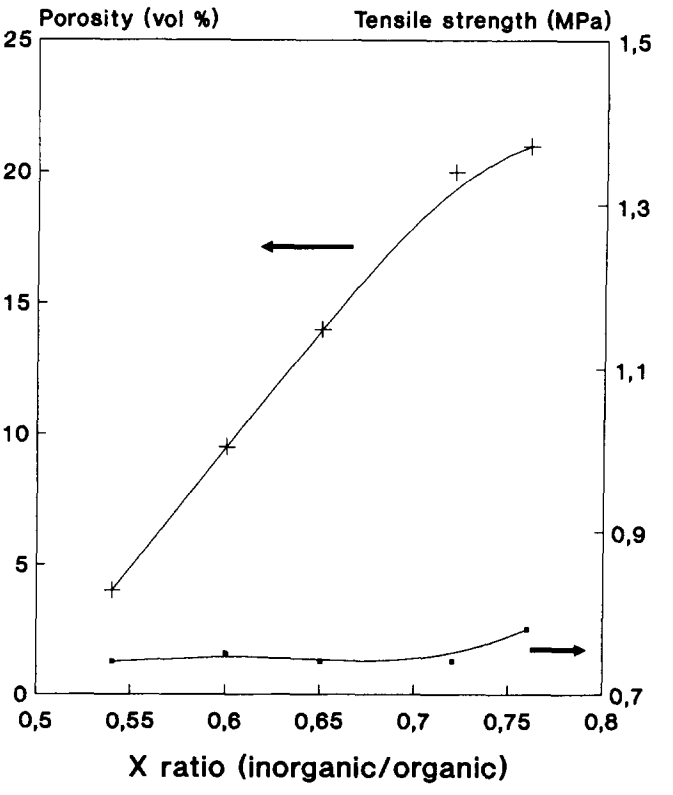

Fig. 8. Tensile strength and porosity of green tapes versus X (grade B).

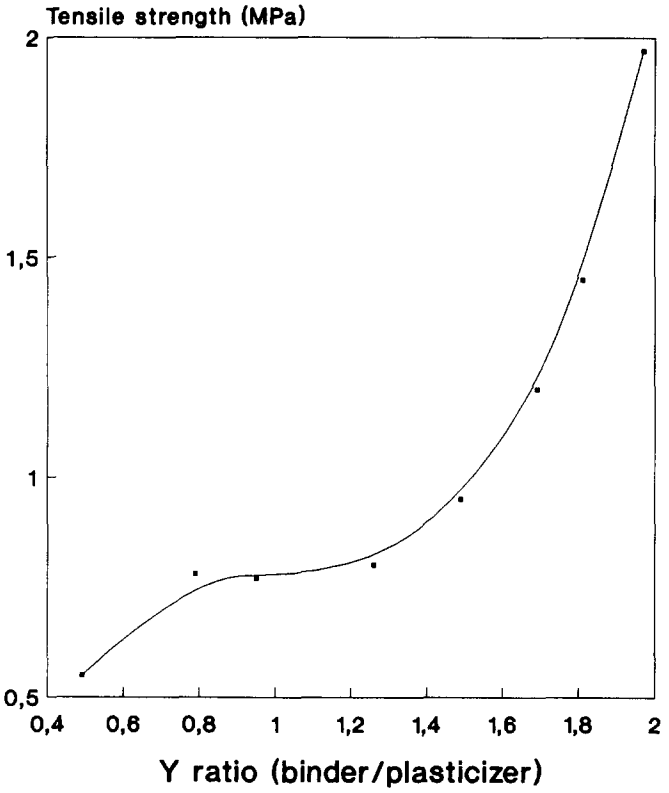

Fig. 9. Tensile strength of green tapes versus *Y* (grade B).

3.2 Sintering study

3.2.1 Densification

The values of density, open porosity and crystallographic nature of intergranular phases of products sintered at 1650°C are given in Table 7. A low open porosity (<1%) was considered to be associated with a high densification.

When $CaCO_3$ is the sintering aid, liquid forms at a temperature as low as 1400°C in the $CaO–Al_2O_3$ system. This liquid solidifies into $CaAl_2O_4$ aluminate. A low amount of $CaCO_3$ (<0·5%) was enough to yield dense AlN materials (open porosity <0·1%).

CS, C3S3A or CS2A lead to the formation of liquids at temperatures of 1400, 1587, 1600 and 1553°C in the systems $CaO–Al_2O_3$, $CaO–SiO_2$, $SiO_2–Al_2O_3$ and $CaO–SiO_2–Al_2O_3$, respectively. CS and CS2A are not as efficient as C or C3S3A, and higher contents were necessary to yield a low porosity. Typical values were between 0·5% and 1% for C but between 2% and 4% for CS.

3.2.2 Thermal properties

The thermal conductivity (k, in $W m^{-1} K^{-1}$) of sintered samples is expressed by eqn (6):

$$k = a d_0 Cp \tag{6}$$

where a is thermal diffusivity, d_0 is density, and Cp is heat capacity.

The heat capacity of sintered samples was not measured. The heat capacity value may slightly vary with the nature and the amount of additives, even in the concentration range used (<6 wt%), and cannot be considered equal to the heat capacity value of pure, dense aluminum nitride (0·734 $J g^{-1} K^{-1}$ at 20°C). Therefore thermal conductivity has not been calculated and only the thermal diffusivity values are reported.

Table 8 shows that thermal diffusivity depends on the nature and concentration of sintering aids:

(i) For the C additive thermal diffusivity begins to increase as the additive content increases, then reaches a maximum for 1·5% of C, then decreases gradually. It must be pointed out that the maximum in thermal diffusivity was not observed at the same additive content as the maximum in apparent density (<0·5%).

(ii) For CS, C3S3A and CS2A thermal diffusivity begins to increase as the additive content increases, then reaches a maximum for 2% of

Table 7. Apparent density (d, $g cm^{-3}$), open porosity (P_0, vol.%) and nature of intergranular phases in AlN materials with various additives sintered at 1650°C

Additive content (wt%)	*Composition*									
	C–AlN		*CS–AlN*		*C3S3A–AlN*		*CS2A–AlN*		*Y_2O_3–AlN*	
	d	P_0	d	P_0	d	P_0	d	P_0	d	P_0
0·5	3·22	0·1	3·08	1·5	3·25	0	—	—	—	—
1	3·20	0·3	3·10	0·5	3·24	0	—	—	—	—
1·5	3·19	0·7	3·15	0·3	3·23	0·1	—	—	—	—
2	3·17	0·5	3·21	0·3	3·22	0·1	3·13	3	2·60	20
4	3·05	0·6	3·18	0·1	3·20	0·4	3·24	0·2	2·67	16
6	2·84	3	3·15	0·3	3·11	2·5	3·23	0·1	2·70	15
Intergranular phases	$CaAl_2O_4$		$CaAl_4O_7$ and/or $Ca_3Al_{10}O_{18}$ $Ca_2SiAl_2O_7$		$CaAl_4O_7$ and/or $Ca_3Al_{10}O_{18}$ 27R AlN-polytype		$CaAl_4O_7$ and/or $Ca_3Al_{10}O_{18}$ 27R AlN-polytype		$Y_3Al_{15}O_{12}$	

Table 8. Influence of additives on thermal diffusivity (a) of AlN

Composition		*Additive content (wt%)*					
		0·5	*1*	*1·5*	*2*	*4*	*6*
C–AlN	a ($cm^2 s^{-1}$)	0·25	0·26	0·30	0·26	0·24	0·12
	P_0 (vol.%)	0·1	0·25	0·7	0·5	0·6	3
CS–AlN	a ($cm^2 s^{-1}$)	0·16	0·18	0·19	0·21	0·21	0·18
	P_0 (vol.%)	1·5	0·5	0·3	0·3	0·1	0·3
C3S3A–AlN	a ($cm^2 s^{-1}$)	0·25	0·23	0·22	0·22	0·19	0·16
	P_0 (vol.%)	0	0	0·1	0·1	0·4	2·5
CS2A–AlN	a ($cm^2 s^{-1}$)	n.d.	n.d.	n.d.	0·19	0·20	0·16
	P_0 (vol.%)	n.d.	n.d.	n.d.	3	0·2	0·1
Y_2O_3–AlN	a ($cm^2 s^{-1}$)	n.d.	n.d.	n.d.	0·23	0·27	0·32
	P_0 (vol.%)	n.d.	n.d.	n.d.	20	16	15

CS, 0·5% of C3S3A and 4 wt% of CS2A, then decreases. The maximum in diffusivity, however, corresponds to the maximum in apparent density.

(iii) For Y_2O_3 thermal diffusivity also increases with the additive content, though the porosity value does not vary between 4 and 6 wt% Y_2O_3.

The content of additive which leads to the highest thermal diffusivity for the C–AlN material (1·5 wt%) is greater than the content which leads to the highest density (0·5 wt%). The thermal diffusivity of Y_2O_3–AlN increased, although the density remained constant. This shows that intergranular phases can have a positive influence on the thermal diffusivity of sintered materials. It is thought that, in both cases, the eutectic liquid cleans the surface of AlN grains, therefore prevents oxygen from entering the AlN lattice.[16] For excessive contents of additive, however, the diffusivity decreases due to the presence of thermal barriers associated with secondary-phase segregations. TEM was used to study materials with 2% and 6% of C and CS additions. For low additive concentrations (2%) secondary phases are segregated at triple points (Fig. 10(a)) and the grain boundaries are free of segregations. In that situation the secondary phases do not scatter phonons severely. For higher additive contents (6%) secondary phases are segregated both at triple points and along grain boundaries (Fig. 10(b)). The secondary phases around the grains diffuse phonons severely. For C3S3A–AlN and CS2A–AlN materials the 27R polytype could be a supplementary cause for the degradation of thermal diffusivity.[26]

3.2.3 Thermal properties of secondary phases

Secondary phases were synthesized in order to determine their intrinsic thermal diffusivity. Apparent and true density, open porosity and variations of thermal diffusivity are given in Table 9.

The $CaAl_4O_7$, $Ca_3Al_{10}O_{18}$ and $Y_3Al_5O_{12}$ compounds were poorly densified at 1680°C, with open porosities of the order of 10%, whereas the $CaAl_2O_4$, $Ca_2SiAl_2O_7$ and Al_2O_3 compounds were

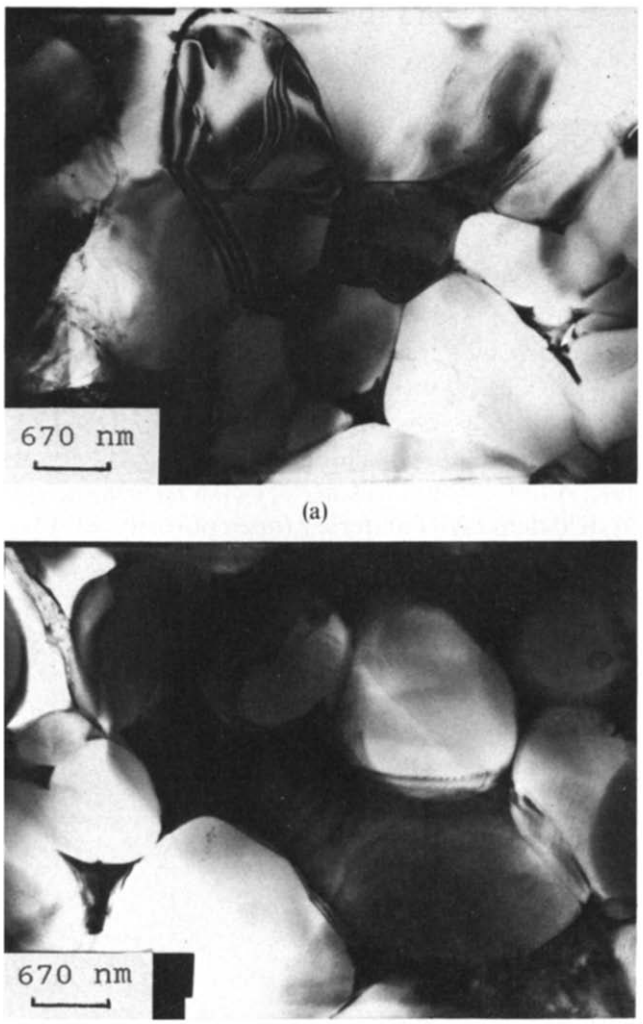

Fig. 10. TEM observations: (a) 2 wt% $CaCO_3$; (b) 6 wt% $CaCO_3$.

Table 9. Characteristics of secondary phases

	Secondary phase					
	$Ca_2SiAl_2O_7$	$CaAl_2O_4$	$Ca_3Al_{10}O_{18}$	$CaAl_4O_7$	$Y_3Al_5O_{12}$	Al_2O_3
d (g cm^{-3})	2·81	2·84	2·58	2·44	3·89	3·91
P_0 (%)	2·0	3·4	8·9	12·5	11·4	0·3
d_{th}	2·96	3·22	3·38	3·44	4·50	3·97
a	← Increasing thermal diffusivity →					

well densified, with open porosities of only 0·3% and 3·4%. Neglecting the variations of density, it can be seen that all the aluminates exhibit a lower thermal diffusivity than alumina. However, the $Y_3Al_5O_{12}$ phase exhibits a higher thermal diffusivity than other compounds, which confirms that yttria is more favorable than other additives from this point of view. The thermal diffusivity of the $CaAl_2O_4$ phase (formed in C–AlN) is lower than those of $CaAl_4O_7$ and $Ca_3Al_{10}O_{18}$ phases (formed in the CS–AlN, C3S3A–AlN and CS2A–AlN). The use of CS, C3S3A and CS2A additives leads to the formation of $Ca_2SiAl_2O_7$ and/or 27R AlN polytype phases. These phases have a very low diffusivity, which is the cause for a severe drop in the diffusivity of the corresponding AlN materials.

4 Conclusion

This work has shown that the organic components in a slurry play a prominent role on the green properties of tape cast materials. The influence of three parameters, namely the inorganic to organic ratio (X), the binder to plasticizer ratio (Y) and the mean grain size of the powder (ϕ), was studied. The results show that a compromise must always be found:

(i) A high apparent density requires a high value of X, whereas a high resistance to cracking and a good thermocompression ability require a low value of X.
(ii) A high apparent density and an absence of cracking require a low value of Y, whereas a good thermocompression ability and a high strength require a high value of Y.
(iii) Particles of medium size (around 2 μm) lead to a high apparent density and good cracking resistance.

Nearly dense AlN substrates can be produced by a sequence of tape casting, thermocompression and sintering. $CaCO_3$ and $3CaO–3SiO_2–Al_2O_3$ are efficient sintering aids, which act as a concentration of 0·5% to lead to dense materials after sintering at 1650°C.

The thermal diffusivity of sintered materials depends on the thermal diffusivities and distribution of intergranular phases.[27] The additive forms a liquid which cleans the surface of the nitride grains, thereby preventing oxygen from entering the AlN lattice. However, the additive concentration must be low for all the secondary phase to remain at the triple points. When too high a content of additive is used the wetting of grains by secondary phases results in a drop in diffusivity. Other additives are less favorable than $CaCO_3$ because they give low-diffusivity phases.

Acknowledgements

The authors thank Dr M. A. Bettinelli (XERAM, Pechiney, France) for his help in preparing the AlN samples and Drs M. F. Denanot and J. Rabier (University, Poitiers, France) for their TEM observations.

References

1. Chartier, T., Streicher, E. & Boch, P., Phosphate esters as dispersants for the tape casting of alumina. *Am. Ceram. Soc. Bull.*, **66** (1987) 1653–5.
2. Morris, J. R. & Cannon, W. R., Rheology and component interactions in tape casting slurries. In *Materials Research Society Symposium Proceedings*, Vol. 60. Mat. Res. Soc., Pittsburgh, PA, 1986, pp. 135–42.
3. MacKinnon, R. J. & Blum, J. B., Particle size distribution effects on tape casting of barium titanate. In *Advances in Ceramics, Vol. 9: Forming in Ceramics*, ed. J. A. Mangels. The Am. Ceram. Soc., Columbus, Ohio, 1984, pp. 150–7.
4. Fiori, C. & de Portu, G., Tape casting: a technique for preparing and studying new materials. *Br. Ceram. Proc.*, **38** (1986) 213–25.
5. Mistler, R. E., Shanefield, D. J. & Runk, R. B., Tape casting of ceramics. In *Ceramic Processing before Firing*, ed. G. Y. Onoda Jr & L. L. Hench. John Wiley & Sons, New York, 1978, pp. 411–18.
6. Shanefield, D. J., Tape casting for forming advanced ceramics. In *Encyclopedia of Materials Science and Engineering*, ed. M. B. Bever. Pergamon Press, Oxford, 1984, pp. 4855–8.

7. Mikeska, K. & Cannon, W. R., Dispersant for tape casting pure barium titanate. In *Advances in Ceramics, Vol. 9: Forming in Ceramics*, ed. J. A. Mangels. The Am. Ceram. Soc., Columbus, Ohio, 1984, pp. 164–83.
8. Williams, J. C., Doctor Blade Process. In *Treatise on Material Science and Technology, Vol. 9: Ceramics Fabrication Processes*, ed. F. F. Y. Wang. Academic Press, New York, 1976, pp. 173–97.
9. Braun, L., Morris, Jr J. R. & Cannon, W. R., Viscosity of tape-casting slips. *Am. Ceram. Soc. Bull.*, **64**(5) (1985) 727–9.
10. Structure–propriétés–mises en oeuvre et normalisation. In *Précis de Matière Plastique*, ed. J. P. Trotignon, M. Piperaud, J. Verdu & A. Dobraczynski. Nathan, Paris, France, 1985, pp. 20–1.
11. Herring, C., Effect of change of scale on sintering phenomena. *J. Appl. Phys.*, **21**(5) (1950) 301–3.
12. Komeya, K. & Inoue, H., Sintering of aluminum nitride: particle size dependence of sintering kinetics. *J. Mat. Sci.*, **4** (1969) 1045–50.
13. Vissokov, G. P. & Brakalov, L. B., Chemical preparation of ultrafine aluminum nitride by electric-arc plasma. *J. Mat. Sci.*, **18**(7) (1983) 2011–16.
14. Gauthier, G., Etude phénoménologique du frittage d'une poudre agglomérée: le nitrure d'aluminium. Thesis, University of Limoges, France, April 1986.
15. Kurokawa, Y., Ustumi, K., Takamizawa, H., Kamata, T. & Noguchi, S., AlN substrates with high thermal conductivity. *IEEE Trans. Comp. Hyb. Manuf. Technol., CHMT*, **8**(6) (1985) 247–52.
16. Anzai, K., Iwase, N., Shinozaki, K. & Tsuge, A., Development of high thermal conductivity aluminum nitride substrates materials by pressureless sintering. *Proc. 1st IEEE CHMT Symp. Tokyo*, Vol. 10. Components, Hybrid and Manufacturing Technology Soc., 1984, pp. 23–8.
17. Komeya, K. & Inoue, H., The influence of fibrous aluminum nitride on the strength of sintered AlN–Y_2O_3. Trans. J. Brit. Ceram. Soc., **70** (1971) 107–13.
18. Komeya, K., Inoue, H. & Tsuge, A., Role of Y_2O_3 and SiO_2 additions in sintering of AlN. *J. Am. Ceram. Soc.*, **54**(9) (1974) 411–12.
19. Yefsah, S., Frittage naturel du nitrure d'aluminium et propriétés des frittés. Thesis, University of Limoges, France, February 1984.
20. Yefsah, S., Billy, M., Jarrige, J. & Mexmain, J., Réalisation de pièces céramiques en nitrure d'aluminium par frittage classique. *Rev. Int. Htes Temp. Réfract. Fr.*, **18**(2) (1981) 167–72.
21. Komeya, K., Tsuge, A., Inoue, H. & Ohta, H., Effects of $CaCO_3$ addition on the sintering of AlN. *J. Mat. Sci. Lett.*, **1**(8) (1986) 325–6.
22. Figure 5141, *Phase Diagrams for Ceramists, Vol. IV*, ed. G. Smith. The Am. Ceram. Soc., Columbus, Ohio, 1981.
23. Dong, C. & Bowen, H. K., Hot-stage study of bubble formation during binder burnout. *J. Am. Ceram. Soc.*, **72**(6) (1989) 1082–7.
24. Cima, M. J., Lewis, J. A. & Devoe, A. D., Binder distribution in ceramic greenware during thermolysis. *J. Am. Ceram. Soc.*, **72**(7) (1989) 1192–9.
25. Lewis, J. A. & Cima, M. J., Diffusivities of dialkyl pthalates in plasticized poly(vinyl butyral): Impact on binder thermolysis. *J. Am. Ceram. Soc.*, **73**(9) (1990) 2702–7.
26. Yagi, T., Shinozaki, K., Ishizawa, N., Mizutani, N. & Kato, M., Effect of silicon dioxide on the thermal diffusivity of aluminum nitride ceramics. *J. Am. Ceram. Soc.*, **71**(7) (1988) C-334–C-338.
27. Russel, C., Hofmann, T. & Limmer, G., Thermal conductivity of aluminum nitride ceramics. *Ceramic Forum Int.*, **1/2** (1991) 22–6.